The Role of Water on the Oxidation Process of Graphene Oxide Structures

Kürşat Kanbur[1,2] (iD), Işıl Birlik[3,4*] (iD), Fatih Sargın[1,2] (iD), N. Funda Ak Azem[3,4] (iD), Ahmet Türk[2] (iD)

[1]Dokuz Eylul University, The Graduate School of Natural and Applied Sciences, Department of Metallurgical and Materials Engineering, İzmir, Türkiye, kursat.kanbur@cbu.edu.tr, fatih.sargin@cbu.edu.tr
[2]Manisa Celal Bayar University, Faculty of Engineering and Natural Sciences, Department of Metallurgical and Materials Engineering, Manisa, Türkiye, kursat.kanbur@cbu.edu.tr, fatih.sargin@cbu.edu.tr, ahmet.turk@cbu.edu.tr
[3]Dokuz Eylul University, Faculty of Engineering, Department of Metallurgical and Materials Engineering, İzmir, Türkiye, isil.kayatekin@deu.edu.tr, funda.ak@deu.edu.tr
[4]Dokuz Eylul University, The Graduate School of Natural and Applied Sciences, Department of Nanoscience and Nanoengineering, İzmir, Türkiye, isil.kayatekin@deu.edu.tr, funda.ak@deu.edu.tr
*Corresponding Author

ARTICLE INFO

ABSTRACT

Graphene oxide (GO) has recently attracted attention with its unique chemical and physical properties and serves as a raw material for graphene-based materials. GO has been produced for decades by the Hummers Method with the oxidation process of graphite. The properties and structure of GO are significantly affected by the production parameters of Hummers Method. In this study, the effect of the water content on the oxidation level of GO structure was investigated. GO was produced with different amounts of water in the oxidation stage of Hummers Method. The structural characterizations of produced GO were carried out by X-ray Diffraction Technique (XRD), Fourier Transform Infrared Spectroscopy (FTIR), X-ray Photoelectron Spectroscopy (XPS), Energy Dispersive X-ray Spectroscopy (EDS), UV-Visible Spectroscopy (UV-Vis) and Raman Spectroscopy. Additionally, morphological and thermal characterization of the produced GO samples were performed by Scanning Electron Microscopy (SEM) and Thermogravimetric Analysis (TGA)/Differential Thermal Analysis (DTA), respectively. According to XRD, FTIR, XPS, and EDS results, it was determined that the oxidation degree of GO decreased with increasing amount of water. Besides, it was revealed that the post-oxidation step generated more defects in the basal plane of graphene according to the results of the Raman Analysis. Also, it was observed that GO had a smoother surface and was found to have higher thermal stability with increasing amounts of water. The results show that the post-oxidation step reduces the oxidation degree of GO, increases the amount of the defect, provides a less wrinkled structure, and improves the thermal stability of GO.

1. Introduction

Graphene is a two-dimensional honeycomb lattice structure consisting of sp^2 hybridized carbon atoms [1, 2]. Graphene is one of the most important candidates for high-tech applications due to its advanced mechanical, electrical, optical, and thermal properties [3, 4]. However, various functional groups are required for some special applications such as sensors [5], filters [6], and biomaterials [7]. GO, a single layer of graphene nanosheets functionalized by several oxygen-containing groups has been synthesized via oxidation of graphite into graphitic oxide followed by exfoliation [8, 9]. It has remarkable physical and chemical properties which makes it a sought-after material for applications in areas that include electronics, biomedicine, energy, and the environment.

GO stands out in the production of chemically modified graphene because it is easy to functionalize with a wide variety of functional groups [10-12]. The functional groups are placed on the graphene planes by oxidation of the graphite basal planes during GO production. As these functional groups are bonded to the basal plane, the carbon atoms perform sp^3 hybridization at the location of the functional groups [13]. Thus, the conductivity of the GO structure decreases as the oxidation degree increases, since the excess electrons are used to bond with the functional groups.

Under extreme oxidation conditions, these functional groups can bind to the carbon basal plane and the carbon basal plane is distorted. However, these functional groups provide hydrophilic properties for GO structures and GO structures are dissolved in a variety of organic and water-based solutions. Thus, GO structures are easily used as reinforcement or matrix material in nanocomposite production for various applications by forming stable colloids [2]. Also, the properties of GO structures can be changed by adjusting the oxidation degree or various modifications [14].

GO production with the chemical oxidation of graphite provides large-scale productivity and efficiency [15]. The production of GO begins with the intercalation between graphite layers and proceeds with the oxidation of graphite layers in the chemical oxidation procedure. The first known work on the oxidation of graphite was made by Benjamin Brodie [16]. The Brodie method was evolved by Staudenmaier in 1898 by reducing the amount of HNO_3 (oxidizing agent) and adding sulfuric acid (H_2SO_4) instead of HNO_3 [10].

In the Staudenmaier method, the release of toxic gases has decreased compared to the Brodie method thanks to the lower amount of HNO_3. However, the Staudenmaier method was still a dangerous process due to the release of toxic gases. Therefore, a safer chemical oxidation method was found by Hummers and Offeman in 1958 [17] and it became the most widely used method for GO production. Hummers method has advantages in terms of reaction time than previous methods. However, there are emissions of nitrogen-based toxic gases (NO_2 and N_2O_4) due to $NaNO_3$. The Hummers Method was developed by Marcano et al [18] in 2010 and named as Improved Hummers Method. This method has a higher degree of oxidation and a better-quality structure with fewer defects for GO compared to previous methods. Various modifications have been made to Hummers method in the literature for optimization and adjusting controllable structure for GO production [14, 19].

According to the literature, the first oxidation stage is started by adding $KMnO_4$ after graphite is mixed with a mixture of H_2SO_4 and H_3PO_4 acid. After the solution is mixed at a certain time and temperature, the post-oxidation stage is initiated by adding water. However, many studies apply different processes in the post-oxidation stage. Hummers and Offeman used 4.6 liters of water for 100 g graphite and mixed it to the graphite-acid solution at 98°C for only 15 minutes [17]. Eigler et al. [11], 60 ml water was mixed with 1 g graphite for 2 hours at 10°C.

Cote et al. [20], mixed 80 ml water for 2 g graphite at 90°C for 1 hour. In 2015, Kang J. H. et al. [21] examined different times and temperatures in the post-oxidation stage. Accordingly, as the temperature increases, the hydroxyl, carbonyl, and carboxyl functional groups ratios of GO are increased. Also, conversion of epoxy groups to hydroxyl-containing groups in GO structure has been found. However, no study has been found in the literature on the effect of the amount of water in the post-oxidation stage on the GO structure.

In this study, GO structures were successfully synthesized by carefully controlling the amount of water in the post-oxidation stage and the effect of the water content during the production stage on the oxidation level of GO has been systematically investigated.

2. Materials and Method

Graphite powder (average powder size <20 μm) was purchased from Sigma Aldrich. H_2SO_4 (95-97%), H_3PO_4 (85%), $KMnO_4$ (99%), and H_2O_2 (35%) were obtained from Isolab Chemicals. All chemicals were used as received without further

purification. GO was produced by using Improved Hummers Method from pure graphite powder. Briefly, 1 g graphite was stirred in 100 ml H_2SO_4:H_3PO_4 acid solution at a ratio of 9:1 to provide pre-oxidation. The first oxidation step was initiated by adding 6 g $KMnO_4$ as the oxidizing agent. (H_2SO_4:H_3PO_4)/Distilled water volume ratio was then determined as 1:0.5, 1:1 and 1:1.5 ml to determine the effect of water content in the forthcoming oxidation step, and the samples were designated as W1, W2, and W3, respectively. Sample without water content was also prepared as W0 for comparison the effect of water content in the post-oxidation stage. H_2O_2 was used to stop oxidation reaction.
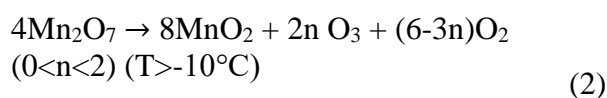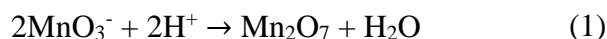
The resulting product was left to precipitate overnight, and the supernatant was discarded. The obtained product was washed three times with HCl solution to remove impurities. The GO was then washed with distilled water until the pH of the solution was neutral. Centrifugation was performed to separate the supernatant at each wash step (NF1200R, Nuve). Finally, the remaining product was dried overnight to obtain GO sample. Structural, morphological, and thermal characterizations were performed to determine the structure and the effect of different water contents during oxidation stages on the properties of GO. For this purpose, X-ray diffraction (XRD) analysis with Cu-K_α radiation (λ=0.154 nm) was performed to determine the oxidation degree and interlayer distance of the GO.

Fourier Transform Infrared Spectroscopy (FTIR) analysis was performed using the Thermo Scientific FTIR Spectrometer with an attenuated total reflection (ATR) module to identify functional groups on the GO basal planes. Also, absorbance of functional groups was determined according to water amount to define the effect of oxidation stage. Thermo Scientific K-Alpha XPS was performed to determine the types and amounts of elemental bonds of the GO structure. In XPS analysis, Al-K_α radiation was measured with 0.1 eV energy step size. The obtained peaks were deconvoluted with Gaussian fitting after Shirley background subtraction. SEM analysis (Zeiss GeminiSem 500) was performed to determine the effect of oxidation step on the morphological structure of GO. UV-Vis analysis
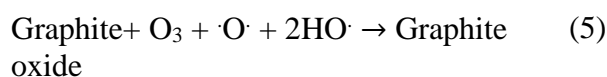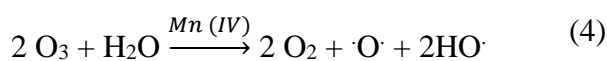
(Thermo Scientific Evolution 260 BIO UV Spectrophotometer) was carried out to specify the sp^2-conjugation on the GO basal plane. DTA/TGA analysis was carried out to determine the thermal properties of the produced GO structures. Analysis was carried out in a Shimadzu DTG 60-H instrument up to 900°C with a heating rate of 2°C/min under nitrogen atmosphere. Micro-Raman analysis was performed with Renishaw In Via Confocal Raman Microscope to investigate defects in the GO samples (532 nm laser and 2400 l/mm).
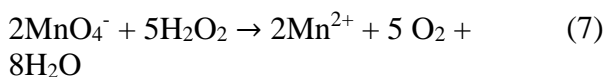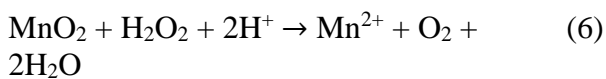
3. Results and Discussion

The oxidation stage begins with the addition of $KMnO_4$ to graphite-acid solutions. Dimanganese heptoxide (Mn_2O_7) and permanganate cation (MnO_3^+) are formed with H^+ ions in the solution (Equation 1) [22]. With the decomposition of Mn_2O_7, O_3 is produced as a by-product (Equation 2). O_3 also oxidizes graphite like Mn_2O_7. This stage is the first oxidation stage in Hummers method. Since the oxidation process is exothermic, homogenous mixing is necessary to avoid local overheating in the container. After this stage, post-oxidation stage begins with addition of water.

$$2MnO_3^- + 2H^+ \rightarrow Mn_2O_7 + H_2O \qquad (1)$$

$$4Mn_2O_7 \rightarrow 8MnO_2 + 2n\ O_3 + (6-3n)O_2$$
$$(0<n<2)\ (T>-10°C) \qquad (2)$$

It is generally recommended to keep the temperature below 60°C to control the temperature and prevent foaming [23]. Adding water to the medium quenches Mn_2O_7 and permanganate acid is formed ($HMnO_4$) (Equation 3) [23]. During this step, oxidation is carried out by permanganate (MnO_4^-) in acidic aqueous solution with various manganese (VII) containing oxo-species. The proposed mechanism was shown in equations 4 and 5 [24].

$$Mn_2O_7 + H_2O \rightarrow 2\ HMnO_4 \qquad (3)$$

$$2\ O_3 + H_2O \xrightarrow{Mn\ (IV)} 2\ O_2 + \cdot O\cdot + 2HO\cdot \qquad (4)$$

$$\text{Graphite} + O_3 + \cdot O\cdot + 2HO\cdot \rightarrow \text{Graphite oxide} \qquad (5)$$

However, when H_2O_2 is added without any water addition, second oxidation step is skipped. [21]. In the last step, manganese compounds present in the solution converted to manganese ions by H_2O_2 (Equation 6 and 7) [23]:

$$MnO_2 + H_2O_2 + 2H^+ \rightarrow Mn^{2+} + O_2 + 2H_2O \qquad (6)$$

$$2MnO_4^- + 5H_2O_2 \rightarrow 2Mn^{2+} + 5\,O_2 + 8H_2O \qquad (7)$$

The XRD results of graphite and GO samples are given in Figure 1. According to the XRD analysis of graphite, the characteristic peak belonging to the (002) plane was detected at 26.60° [25]. The peak belonging to the (004) plane of graphite was also found at 54.40°. Besides, the other peaks (42.3, 44.4, 54.4, 77.5 and 83.5) are generally located in the graphite phase. The whole structure was determined to consist of graphite phase with high crystallinity [26]. The 2θ values of W0, W1, W2 and W3 samples are 10.2º, 11.56º, 11.96º and 12.24º, respectively. The peak around 2θ=11° is the characteristic peak of the GO structure associated with (001) plane [25].

According to the results, the 2θ angle of the characteristic (001) plane shifts to a higher angle with the increasing water content. The interlayer distance values (d) of GO was calculated according to the Bragg's Law [27] and listed in Table 1. The interlayer distance of graphite, W0, W1, W2 and W3 samples are 3.348, 8.665, 7.648, 7.393 and 7.225 Å, respectively. The functional groups are formed during oxidation process and so it increases the interlayer distance of graphite layers. All samples produced with different water content has higher interlayer distance than the graphite interlayer distance (3.34 Å), which demonstrates the successful oxidation process. In addition, it was found that the oxidation degree decreases with the increasing water amount due to the increase in the interlayer distances. In a study, it was noted that adding more than 4 ml of water reduces the interlayer distance of GO layers [24].

Tour M. et. al. [28] specified that too much dilute acid solution reduces oxidation of graphite. In another study [10], it was stated that with the addition of water in the second oxidation step,

Mn_2O_7 is quenched and transformed into MnO_4^-. It was pointed out that the Mn_2O_7 was more oxidizing than MnO_4^-. Therefore, as the oxidation degree reduced with the increasing amount of water, functional groups were decreased at interlayer distances of GO. Accordingly, the characteristic peak of GO was shifted to the higher angle. Also, it was interpreted that the characteristic peak of the graphite (002) plane, which is around 26.6°, is observed in the XRD result of the W3 sample [29]. It was determined that the unexfoliated graphite structure was still present in the W3 sample and the oxidation conditions were not sufficient to oxidize all the graphite for W3 sample. Therefore, it was figured out that there was not enough oxidizing condition in W3.
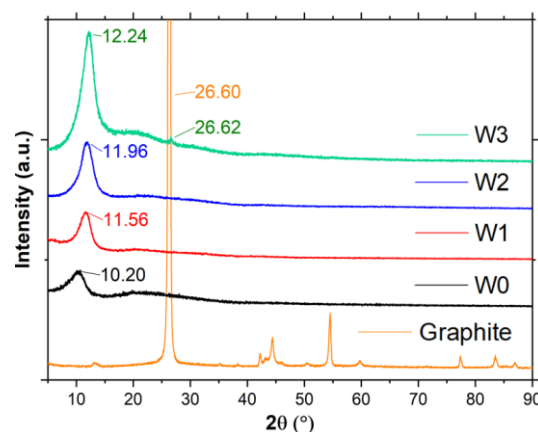

Figure 1. XRD analysis of GO samples produced with different water content

Table 1. Interlayer distance of produced GO with different water content

Sample	2θ (°)	d (Å)
Graphite	26.60	3.348
W0	10.2	8.665
W1	11.56	7.648
W2	11.96	7.393
W3	12.24	7.225

FTIR analysis was performed to evaluate the functional groups of GO samples. The FTIR results of GO samples with different water content were given in Figure 2. All samples have characteristic absorbance bands indicating functional groups of GO structure [15]. FTIR results indicated that there were hydroxyl groups (OH) between 3600-2400 cm^{-1}, carbonyl (C=O)

group at 1720 cm^{-1}, stretch mode of C-C bond and absorbed OH groups at 1620 cm^{-1} [30]. Also, 1417 cm^{-1} and 1260 cm^{-1} show symmetrical O-H bending and C-OH stretching in carboxylic acid [31], respectively while 1221 cm^{-1}, 1047 cm^{-1} and 971 cm^{-1} demonstrate O-H bending vibrations in carboxylic acid, C-O-C stretching and axial C-O stretching vibrations, respectively [2, 32, 33].

Also, the absorbance band around 1160 cm^{-1} demonstrates the carboxyl or carbonyl groups in the graphene oxide structures [34]. According to the results, the absorbance of 1620 cm^{-1} and 1260 cm^{-1} absorbance bands slightly increased in the W1, W2 and W3 samples due to the formation of hydroxyl groups originating from the post-oxidation stage (indicated by the arrow) [21]. Therefore, it was determined that the absorbance band associated with the OH functional groups increased with increasing amount of water. In addition, the absorbance of the 1047 cm^{-1} and 1160 cm^{-1} bands increased in the W0 sample and indicates the high oxidation degree of GO (indicated by the arrow) [35].

Moreover, the intensity of 1720 cm^{-1}/1620 cm^{-1} absorbance bands show an increase of oxidation degree for graphene oxide structures [24]. Accordingly, the intensity of 1720 cm^{-1}/1620 cm^{-1} was found highest in the W0 sample by the FTIR results and so these results are consistent with the XRD results.
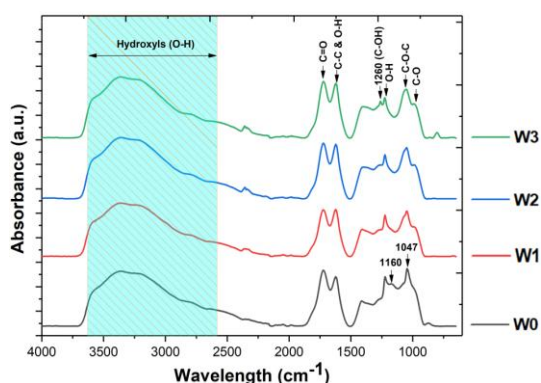

Figure 2. FTIR analysis of GO produced with different water content

XPS is an important analysis method to examine the elemental bonds and chemical states of functional groups in the GO structure. WO and W3 samples were selected for XPS analysis in order to compare the effect of the water on post-oxidation process. C1s and O1s spectrum results of W0 and W3 samples were shown in Figures 3(a) and 3(b) in XPS analysis. According to the obtained results, it is obvious that the carbon bond depicted by C1s intensity of the W0 decreased compared to the W3. In addition, the intensity of the O1s spectrum is dominant for W0 compared to W3 sample. The ratios of C1s and O1s spectra from survey analysis were given in Table 2 for W0 and W3 samples. The C/O ratio was calculated to determine the oxidation degree of GO [29].

According to the results, the C/O ratio is 1.45 for W0 sample and 1.59 for W3 sample, respectively. Therefore, it was observed that the W0 sample had a higher oxidation degree due to its low C/O ratio [29]. Besides, C1s spectrum was deconvoluted to examine in detail for W0 and W3 samples and the results were shown in Figures 3c and 3d. In the deconvolution process, three different functional groups peaks around 284.8, 286.6, 287.8 and 289 indicate C-C/C=C, C-O-C, C=O and O-C=O functional groups, respectively [12, 14, 18]. The ratio of C-C/C=C spectra obtained from deconvolution is 51.98% for the W3 sample and 50.32% for the W0 sample.

Besides, the ratio of spectrums associated with oxygenated functional groups were 49.68% and 48.02% for samples W0 and W3, respectively. The C-C/C=C regions of the W0 sample decreased due to more oxidation [36]. Therefore, the areas of functional groups in the W0 sample increased even more. Moreover, the intensity of the C-O-C epoxy bond is higher in the W0 sample. As the amount of epoxy group increases, the distance between the layers also increases. This situation explains the fact that the interlayer distance is the highest in the W0 sample as a result of XRD. As the temperature of the first oxidation stage is raised, the degree of oxidation increases.

The Mn (VII) compound shows extreme oxidizing properties at high temperatures [24], and so it is understood that the carbon basal plane of the W0 sample is more oxidized. The obtained results are compatible with XRD results due to the lower 2θ values. At the same time, XPS analysis supports the results of FTIR analysis,

since the absorbance of the 1047 cm^{-1} peak is higher for the W0 sample in the FTIR analysis.
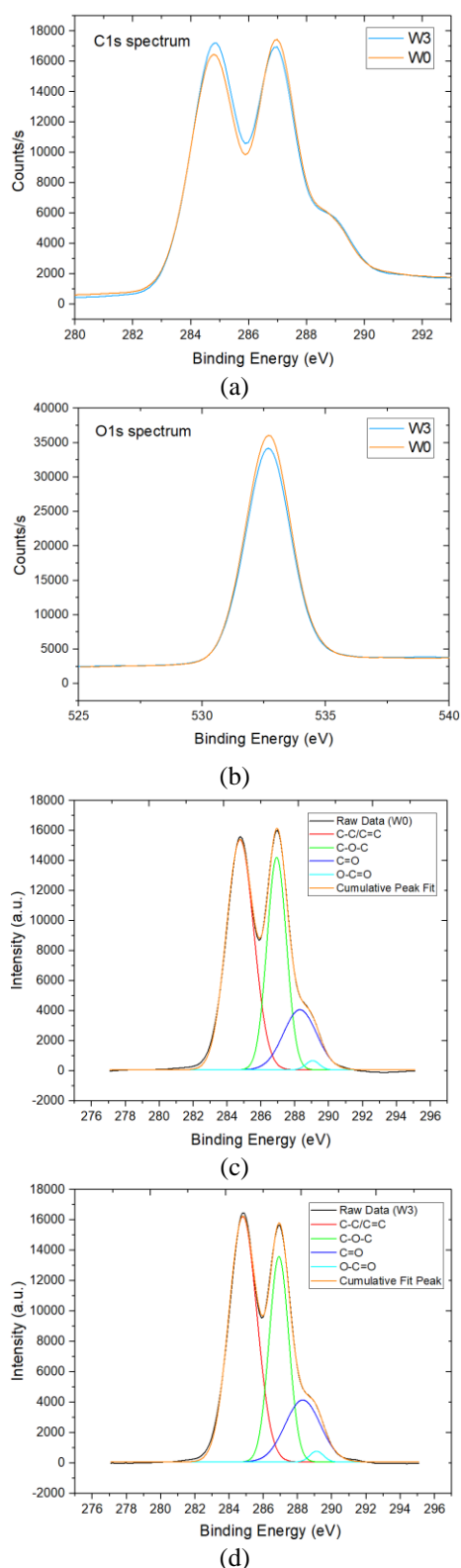

(a)

(b)

(c)

(d)

Figure 3. XPS analysis of GO produced with different water ratios. (a) C1s and (b) O1s spectrum of W0 and W3 samples. Deconvoluted C1s XPS spectrum of (c) W0 and (d) W3 samples

Table 2. Ratio of C1s and O1s results from XPS analyses

Samples	C 1s	O 1s	S 2p	C1s/O1s
W0	57.41	39.49	3.1	1.45
W3	61.40	38.60	-	1.59

SEM analysis is performed to determine the effect of water on the morphology of the samples in the second oxidation step. EDS analysis was carried out to determine the elemental distribution in the produced GO structure. The results of SEM and EDS analysis are shown in Figure 4. According to the results of SEM analysis, all GO structures have folded and crumpled structures. The wrinkled GO surface is due to the addition of functional groups to the graphene basal plane during oxidation [25].

However, a smoother surface is formed as the amount of water increases. As the oxidation conditions increase, the formation of a wrinkled structure is expected. The fluctuation of the GO structure increases with the increasing number of functional groups in the GO structure [37]. Therefore, the W0 sample was observed to undergo high oxidation due to its wrinkled surface structure. In the EDS results, the carbon (C), oxygen (O) and sulfur (S) elements were detected. Graphene oxide structures consist of the C, O, and hydrogen (H) elements. However, H element cannot be detected in the EDS analysis. The element S is included in the structure due to the use of H_2SO_4 in production [38].

Therefore, C and O elements are seen in the EDS analysis. The atomic C/O ratio was calculated to compare the oxidation degree of the GO samples and is shown in the Figure 4. Accordingly, the C/O ratios reached 1.29, 1.48, 1.54 and 1.55 for W0, W1, W2 and W3 samples, respectively. The C/O ratio increased from the W0 sample to the W3 sample. It is known that the C/O ratio in EDX analysis decreases with the increasing oxidation degree of GO [12]. As a result, it was determined that the W0 sample had the highest oxidation degree in the EDX analysis. It is also supported by the EDS analysis result that the degree of oxidation increases with the decreasing amount of water. These results are also compatible with XRD and XPS results.
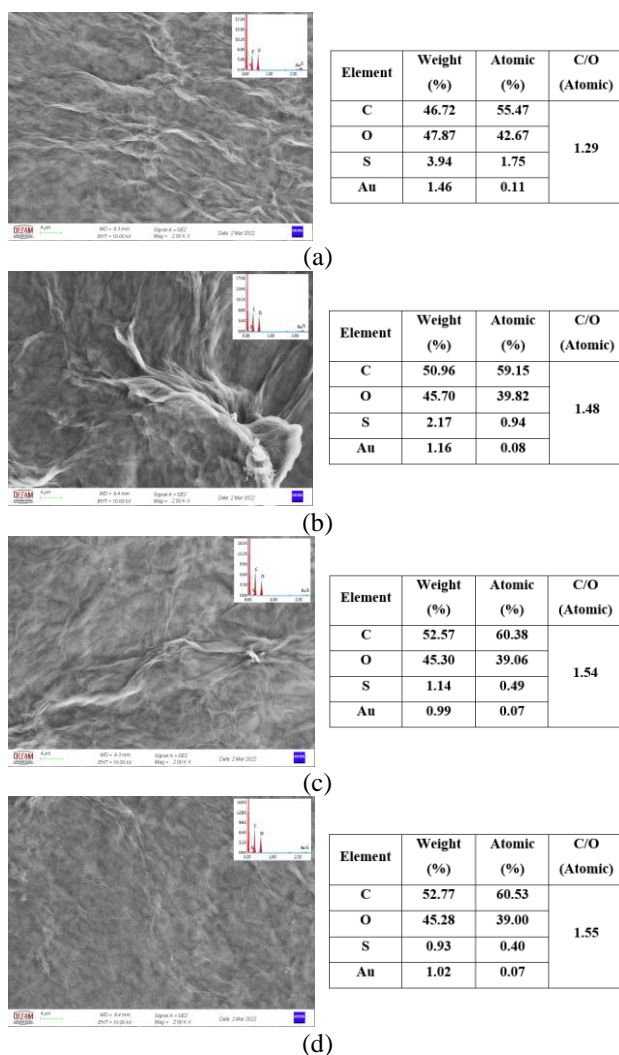
Element	Weight (%)	Atomic (%)	C/O (Atomic)
C	46.72	55.47	
O	47.87	42.67	1.29
S	3.94	1.75	
Au	1.46	0.11	

(a)

Element	Weight (%)	Atomic (%)	C/O (Atomic)
C	50.96	59.15	
O	45.70	39.82	1.48
S	2.17	0.94	
Au	1.16	0.08	

(b)

Element	Weight (%)	Atomic (%)	C/O (Atomic)
C	52.57	60.38	
O	45.30	39.06	1.54
S	1.14	0.49	
Au	0.99	0.07	

(c)

Element	Weight (%)	Atomic (%)	C/O (Atomic)
C	52.77	60.53	
O	45.28	39.00	1.55
S	0.93	0.40	
Au	1.02	0.07	

(d)

Figure 4. SEM and EDS analysis of GO produced with different water ratios. SEM and EDS analysis of (a) W0, (b) W1, (c) W2 and (d) W3 samples

TGA/DTA analysis was performed to determine the thermal decomposition behavior of the produced GO and the results were shown in the Figure 5. According to the result of TGA analysis, a continuous weight loss occurred with increasing temperature in all samples. Weight loss up to 100°C is due to the release of trapped water between the GO layers. At this stage, the W0 sample appears to have the highest moisture content due to the greatest weight loss. The sudden weight loss between about 160-220°C is due to the degradation of unstable oxygen functional groups [12, 39]. For decomposition to occur, the strong interlayer hydrogen bond must be overcome.

Therefore, decomposition is more difficult in samples with more hydrogen bonds. The presence of the newly-OH functional group in the FTIR results of samples with the second

oxidation stage indicates that hydrogen bonding is more in these samples [40]. Therefore, the decomposition temperature also increases with the increasing water amount in the second oxidation stage. In the DTA analysis, an exothermic peak is observed for GO samples between approximately 160 and 200 °C due to the combustion of functional groups [41]. According to the DTA results, the highest decomposition temperature was observed in the W3 sample with 202.86 °C. A gradual loss of mass between about 230 °C and 900 °C is due to the removal of more stable functional groups [24]. At the end of 900 °C, the highest weight loss occurred in the W0 sample, since it has lower hydrogen bonds and more functional groups. Since TGA analysis evaluates in terms of weight loss, it is thought that the structures with the highest weight loss have more functional groups [13].
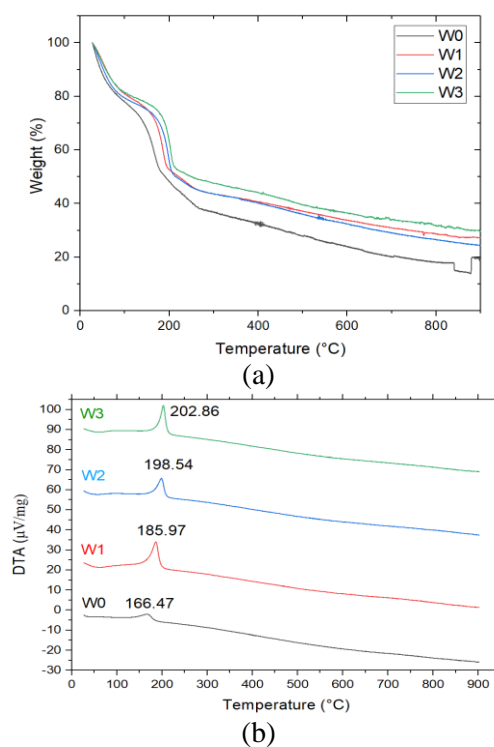

(a)

(b)

Figure 5. (a) TGA and (b) DTA analysis of produced GO with different water ratios

The results of the UV-Vis analysis performed to determine the effect of the post-oxidation step are shown in Figure 6. The UV-Vis spectrum of GO has two characteristic absorbance bands that are used to determine the degree of oxidation of graphene oxide and the amount of sp2 conjugate structure. The absorbance band around 229 nm indicates the $\pi \rightarrow \pi^*$ electron transition of carbon

aromatic bonds (sp2). The second characteristic peak is around 300 nm and was seen as the shoulder. This shoulder indicates the n→π* electron transition of the C=O bond. According to the results, the maximum point of the carbon aromatic bond electron transition of the W0 sample was 226 nm and it was determined that it shifted to the left compared to other samples. This is due to the exfoliation of GO in the post-oxidation step with the increasing oxidation degree [15]. XRD and XPS results also support this situation. As can be seen in the XRD, FTIR and XPS results, the C-C and C=C bond decreased in the W0 sample. Therefore, the W0 sample showed absorbance at the lowest wavelength, since its sp2 conjugate structure also decreased.
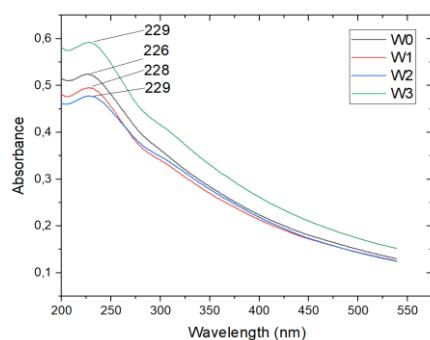

Figure 6. UV-Vis analysis of produced GO with different water ratios

Raman analysis was performed to examine the defects in the structure of GO samples. The Raman analysis results of the samples are shown in the Figure 7. There are two characteristic bands as D and G in Raman Analysis for GO. The D band shows the breathing mode of A_{1g} symmetry in sp2 systems and is around 1350 cm^{-1} band [15, 32]. The G band indicates the E_{2g} phonons at the Brillouin zone center and is around 1590 cm^{-1} band. D and G bands were obtained around 1350 cm^{-1} and 1600 cm^{-1} bands. The shift of the G band may be due to the isolated double bonds after oxidation [29].

To compare the defect rate of GO materials, it is determined by the I_D/I_G ratio using the intensity of the D and G peaks [40, 42]. The I_D/I_G ratios for W0 and W3 samples were 0.82 and 0.84, respectively. In Raman analysis, the D peak increases with the rate of defect or disorder in the graphene plane [40]. Accordingly, more defects

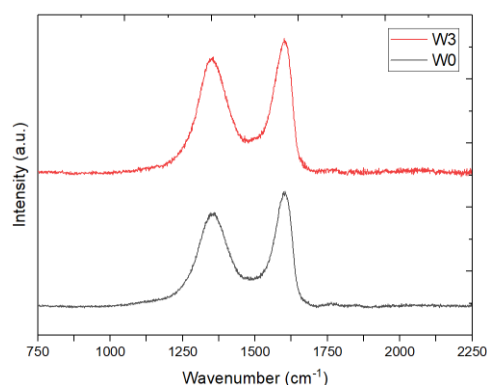were formed in the GO structure with the post-oxidation process.

Figure 7. Raman analysis for W0 and W3 samples

4. Conclusion

GO was successfully produced with the Improved Hummers Method. Effect of water content on the post-oxidation level of GO structure was investigated. The interlayer distance was reduced with the post-oxidation step, and so W0 sample had the highest oxidation degree. The hydroxyl functional group increased in the produced samples with the post-oxidation step. In XPS analysis, the C/O ratio increased from the W0 sample to the W3 sample. In addition, the intensity of the oxygen-containing functional groups is higher for the W0 sample. In the UV-Vis analysis, the W0 sample was detected to have a lower sp^2 conjugate structure.

This indicates that the GO basal plane is excessively oxidized under the W0 sample conditions. According to thermal analysis, the W3 sample was more stable in terms of thermal properties due to lower thermal decomposition temperature. Besides, it was revealed that the highest weight loss occurred in the W0 sample due to the excess of functional groups. Overall results show that the post-oxidation step with increasing water content reduces the oxidation degree of GO, increases defects amount, provides a less wrinkled structure, and improves the thermal stability of GO.

Article Information Form

Fabrication and Application of Electronic Materials for their valuable supports. They would also like to thank Arifmert Cen, Ceyda Otlu, Yunus Emre Demir and Cem İnci for their support in laboratory studies.

Authors' Contribution
The authors contributed equally to the study.

The Declaration of Conflict of Interest/ Common Interest
No conflict of interest or common interest has been declared by the authors.

The Declaration of Ethics Committee Approval
This study does not require ethics committee permission or any special permission.

The Declaration of Research and Publication Ethics
The authors of the paper declare that they comply with the scientific, ethical and quotation rules of SAUJS in all processes of the paper and that they do not make any falsification on the data collected. In addition, they declare that Sakarya University Journal of Science and its editorial board have no responsibility for any ethical violations that may be encountered, and that this study has not been evaluated in any academic publication environment other than Sakarya University Journal of Science.

References

[1] M. P. Araújo, O. S. G. P. Soares, A. J. S. Fernandes, M. F. R. Pereira, C. Freire, "Tuning the surface chemistry of graphene flakes: new strategies for selective oxidation," RSC Advances, vol. 7, no. 23, pp. 14290–14301, 2017.

[2] J. Guerrero-Contreras, F. Caballero-Briones, "Graphene oxide powders with different oxidation degree, prepared by synthesis variations of the Hummers method," Materials Chemistry and Physics, vol. 153, pp. 209–220, 2015.

[3] J. Chen, B. Yao, C. Li, G. Shi, "An improved Hummers method for eco-friendly synthesis of graphene oxide," Carbon, vol. 64, no. 1, pp. 225–229, 2013.

[4] W. S. Koe, J. W. Lee, W. C. Chong, Y. L. Pang, L. C. Sim, "An overview of photocatalytic degradation: photocatalysts, mechanisms, and development of photocatalytic membrane," Environmental Science and Pollution Research, vol. 27, no. 3, pp. 2522–2565, 2020.

[5] T. A. Saleh, G. Fadillah, "Recent trends in the design of chemical sensors based on graphene–metal oxide nanocomposites for the analysis of toxic species and biomolecules," Trends in Analytical Chemistry, vol. 120, 2019.

[6] R. K. Joshi, S. Alwarappan, M. Yoshimura, V. Sahajwalla, Y. Nishina, "Graphene oxide: the new membrane material," Applied Materials Today, vol. 1, no. 1, pp. 1–12, 2015.

[7] D. Ege, A. R. Kamali, A. R. Boccaccini, "Graphene Oxide/Polymer-Based Biomaterials," Advanced Engineering Materials, vol. 19, no. 12, p. 1700627, 2017.

[8] S. Thangavel, G. Venugopal, "Understanding the adsorption property of graphene-oxide with different degrees of oxidation levels," Powder Technology, vol. 257, pp. 141–148, 2014.

[9] Y. Wei, X. Hu, Q. Jiang, Z. Sun, P. Wang, Y. Qiu, W. Liu, "Influence of graphene oxide with different oxidation levels on the properties of epoxy composites," Composites Science and Technology, vol. 161, no. April, pp. 74–84, 2018.

[10] D. R. Dreyer, S. Park, C. W. Bielawski, R. S. Ruoff, "The chemistry of graphene oxide," Chem. Soc. Rev., vol. 39, no. 1, pp. 228–240, 2010.

[11] S. Eigler, S. Grimm, F. Hof, A. Hirsch, "Graphene oxide: a stable carbon framework for functionalization," Journal of Materials Chemistry A, vol. 1, no. 38, p. 11559, 2013.

[12] V. Panwar, A. Chattree, K. Pal, "A new facile route for synthesizing of graphene oxide using mixture of sulfuric-nitric-phosphoric acids as intercalating agent," Physica E: Low-Dimensional Systems and Nanostructures, vol. 73, pp. 235–241, 2015.

[13] M. D. P. Lavin-Lopez, A. Romero, J. Garrido, L. Sanchez-Silva, J. L. Valverde, "Influence of Different Improved Hummers Method Modifications on the Characteristics of Graphite Oxide in Order to Make a More Easily Scalable Method," Industrial & Engineering Chemistry Research, vol. 55, no. 50, pp. 12836–12847, 2016.

[14] D. Yang, A. Velamakanni, G. Bozoklu, S. Park, M. Stoller, R. D. Piner, S. Stankovich, I. Jung, D. A. Field, C. A. Ventrice, R. S. Ruoff, "Chemical analysis of graphene oxide films after heat and chemical treatments by X-ray photoelectron and Micro-Raman spectroscopy," Carbon, vol. 47, no. 1, pp. 145–152, 2009.

[15] S. Eigler, A. M. Dimiev, "Characterization Techniques," in Graphene Oxide: Fundamentals and Applications, A. M. Dimiev and S. Eigler, Eds., United Kingdom: John Wiley & Sons, 2016, pp. 85–118.

[16] B. C. Brodie, "XIII. On the atomic weight of graphite," Philosophical Transactions of the Royal Society of London, vol. 149, no. 1, pp. 249–259, 1859.

[17] W. S. Hummers, R. E. Offeman, "Preparation of Graphitic Oxide," Journal of the American Chemical Society, vol. 80, no. 6, pp. 1339–1339, 1958.

[18] D. C. Marcano, D. V. Kosynkin, J. M. Berlin, A. Sinitskii, Z. Sun, A. Slesarev, L. B. Alemany, W. Lu, J. M. Tour, "Improved synthesis of graphene oxide," ACS Nano, vol. 4, no. 8, pp. 4806–4814, 2010.

[19] F. Boran, S. Çetinkaya Gürer, "The effect of starting material types on the structure of graphene oxide and graphene," Turkish Journal of Chemistry, vol. 43, no. 5, pp. 1322–1335, 2019.

[20] L. J. Cote, J. Kim, Z. Zhang, C. Sun, J. Huang, "Tunable assembly of graphene oxide surfactant sheets: wrinkles, overlaps and impacts on thin film properties," Soft Matter, vol. 6, no. 24, p. 6096, 2010.

[21] J. H. Kang, T. Kim, J. Choi, J. Park, Y. S. Kim, M. S. Chang, H. Jung, K. T. Park, S. J. Yang, C. R. Park, "Hidden Second Oxidation Step of Hummers Method," Chemistry of Materials, vol. 28, no. 3, pp. 756–764, 2016.

[22] A. M. Dimiev, J. M. Tour, "Mechanism of graphene oxide formation," ACS Nano, vol. 8, no. 3, pp. 3060–3068, 2014.

[23] F. J. Tölle, K. Gamp, R. Mülhaupt, "Scale-up and purification of graphite oxide as intermediate for functionalized graphene," Carbon, vol. 75, no. April, pp. 432–442, 2014.

[24] J. Chen, Y. Zhang, M. Zhang, B. Yao, Y. Li, L. Huang, C. Li, G. Shi, "Water-enhanced oxidation of graphite to graphene oxide with controlled species of oxygenated groups," Chemical Science, vol. 7, no. 3, pp. 1874–1881, 2016.

[25] R. Muzyka, M. Kwoka, Ł. Smędowski, N. Díez, G. Gryglewicz, "Oxidation of graphite by different modified Hummers methods," New Carbon Materials, vol. 32, no. 1, pp. 15–20, 2017.

[26] A. A. Muhsan, K. Lafdi, "Numerical study of the electrochemical exfoliation of graphite," SN Applied Sciences, vol. 1, no. 3, p. 276, 2019.

[27] J. Epp, "X-ray diffraction (XRD) techniques for materials characterization," in Materials Characterization Using Nondestructive Evaluation (NDE) Methods, G. Huebschen, I. Altpeter, R. Tschuncky, and H.-G. Herrmann, Eds., Elsevier Inc., 2016, pp. 81–124.

[28] A. L. Higginbotham, D. V Kosynkin, A. Sinitskii, Z. Sun, J. M. Tour, "Lower-Defect Graphene Oxide Nanotubes Nanoribbons from Multiwalled Carbon Nanotubes," ACS nano, vol. 4, no. 4, p. 2059, 2010.

[29] M. F. R. Hanifah, J. Jaafar, M. H. D. Othman, A. F. Ismail, M. A. Rahman, N. Yusof, W. N. W. Salleh, F. Aziz, "Facile synthesis of highly favorable graphene oxide: Effect of oxidation degree on the structural, morphological, thermal and electrochemical properties," Materialia, vol. 6, no. May, p. 100344, 2019.

[30] K. Krishnamoorthy, M. Veerapandian, K. Yun, S.-J. Kim, "The chemical and structural analysis of graphene oxide with different degrees of oxidation," Carbon, vol. 53, pp. 38–49, 2013.

[31] M. Wojtoniszak, D. Rogińska, B. Machaliński, M. Drozdzik, E. Mijowska, "Graphene oxide functionalized with methylene blue and its performance in singlet oxygen generation," Materials Research Bulletin, vol. 48, no. 7, pp. 2636–2639, 2013.

[32] M. J. Yoo, H. B. Park, "Effect of hydrogen peroxide on properties of graphene oxide in Hummers method," Carbon, vol. 141, pp. 515–522, 2019.

[33] S. Thakur, N. Karak, "Green reduction of graphene oxide by aqueous phytoextracts," Carbon, vol. 50, no. 14, pp. 5331–5339, 2012.

[34] V. Ţucureanu, A. Matei, A. M. Avram, "FTIR Spectroscopy for Carbon Family Study," Critical Reviews in Analytical Chemistry, vol. 46, no. 6, pp. 502–520, 2016.

[35] Y. Hou, S. Lv, L. Liu, X. Liu, "High-quality preparation of graphene oxide via the Hummers' method: Understanding the roles of the intercalator, oxidant, and graphite particle size," Ceramics International, vol. 46, no. 2, pp. 2392–2402, 2020.

[36] R. Al-Gaashani, A. Najjar, Y. Zakaria, S. Mansour, M. A. Atieh, "XPS and structural studies of high quality graphene oxide and reduced graphene oxide prepared by different chemical oxidation methods," Ceramics International, vol. 45, no. 11, pp. 14439–14448, 2019.

[37] A. Allahbakhsh, F. Sharif, S. Mazirani, "The Influence of Oxygen-Containing Functional Groups on The Surface Behavior and Roughness Characteristics of Graphene Oxide," Nano, vol. 08, no. 04, p. 1350045, 2013.

[38] S. Eigler, C. Dotzer, F. Hof, W. Bauer, A. Hirsch, "Sulfur Species in Graphene Oxide," Chemistry - A European Journal, vol. 19, no. 29, pp. 9490–9496, 2013.

[39] R. Ikram, B. M. Jan, W. Ahmad, "An overview of industrial scalable production of graphene oxide and analytical approaches for synthesis and characterization," Journal of Materials Research and Technology, vol. 9, no. 5, pp. 11587–11610, 2020.

[40] Q. Zhang, Y. Yang, H. Fan, L. Feng, G. Wen, L. Qin, "Roles of water in the formation and preparation of graphene oxide," RSC Advances, vol. 11, pp. 15808–15816, 2021.

[41] P. S. Narayan, N. L. Teradal, S. Jaldappagari, A. K. Satpati, "Eco-friendly reduced graphene oxide for the determination of mycophenolate mofetil in

pharmaceutical formulations," Journal of Pharmaceutical Analysis, vol. 8, no. 2, pp. 131–137, 2018.

[42] N. Yadav, B. Lochab, "A comparative study of graphene oxide: Hummers, intermediate and improved method," FlatChem, vol. 13, no. February, pp. 40–49, 2019.